

1999

On radio and x-ray emission mechanisms in nearby x-ray bright galactic nuclei

Stephen P. Boughn

Haverford College, sboughn@haverford.edu

Insu Yi

Follow this and additional works at: http://scholarship.haverford.edu/astronomy_facpubs

Repository Citation

"On Radio and X-ray Emission Mechanisms in Nearby X-ray Bright Galactic Nuclei" (with I. Yi), *Ap. J.* 515, 576 (1999).

This Journal Article is brought to you for free and open access by the Astronomy at Haverford Scholarship. It has been accepted for inclusion in Faculty Publications by an authorized administrator of Haverford Scholarship. For more information, please contact nmedeiro@haverford.edu.

ON RADIO AND X-RAY EMISSION MECHANISMS IN NEARBY, X-RAY-BRIGHT GALACTIC NUCLEI

INSU YI¹ AND STEPHEN P. BOUGHN²

Received 1998 June 2; accepted 1998 November 25

ABSTRACT

It has been suggested that advection-dominated accretion flows (ADAFs) are responsible for the X-ray activity in nearby galactic nuclei. These X-ray-bright galactic nuclei (XBGNs) are a heterogeneous group that include LINERs, low- to moderate-luminosity Seyfert galaxies, and narrow-line X-ray galaxies with 2–10 keV X-ray luminosities in the range $\sim 10^{39}$ to $\sim 10^{43}$ ergs s^{-1} . In the absence of a radio jet, the core 15 GHz radio luminosity of an ADAF is relatively low and roughly proportional to the mass of the central black hole. The predicted radio luminosity depends primarily on the black hole mass and for XBGNs typically falls in the range $10^{35} \lesssim L_R \lesssim 10^{39}$ ergs s^{-1} . We designate these as “radio-quiet” XBGNs. However, some level of jet activity seems to be present in most sources and the radio emission can be considerably larger than that from the ADAF core. We discuss connections between radio-bright XBGNs and radio-loud, powerful active galactic nuclei (AGNs) and suggest that the radio activities are directly correlated with black hole spins in both cases. Even in the presence of a radio jet, high-resolution, high-frequency radio imaging of nearby XBGNs could identify compact, inverted-spectrum ADAF radio sources. The unique radio/X-ray luminosity relation is confirmed in a few cases in which black hole masses are known and could be used as a tool to estimate unknown black hole masses. For radio-dim ($L_R \lesssim 10^{39}$ ergs s^{-1}), X-ray-bright ($L_X \gtrsim 10^{43}$ ergs s^{-1}) sources, which are primarily Seyfert galaxies, the X-ray emission mechanism is not accounted for by pure ADAFs and radio activities are likely to be similar to those of the radio-quiet AGNs.

Subject headings: accretion, accretion disks — galaxies: nuclei — radio continuum: galaxies — X-rays: galaxies — X-rays: general

1. INTRODUCTION

It is widely believed that nonstellar emission in galactic nuclei indicates the existence of accreting, massive black holes (e.g., Frank, King, & Raine 1992). It is, however, unclear how to understand the various emission spectra from diverse types of active galactic nuclei (AGNs) powered by accreting black holes (e.g., Osterbrock 1989). Within the luminous AGN population, radio luminosities differ greatly; hence the classification into the radio-loud and radio-quiet subpopulations. The luminous optical/UV/X-ray emission is attributed to accretion flows around massive black holes, while the strong radio emission clearly arises from powerful radio jets.

Recently, it has been suggested that the X-ray and radio emission from less luminous X-ray-bright galactic nuclei (XBGNs) such as LINERs and low-luminosity Seyfert galaxies could be due to optically thin advection-dominated accretion flows (ADAFs) (Yi & Boughn 1998; Di Matteo & Fabian 1997; Fabian & Rees 1995, and references therein). These sources have X-ray luminosities in the range $10^{39} \lesssim L_X \lesssim 10^{43}$ ergs s^{-1} . In ADAFs, low-level radio emission arises from an X-ray-emitting, optically thin plasma via synchrotron emission (e.g., Narayan & Yi 1995b). These sources are characterized by inverted radio spectra and compact emission regions together with hard X-ray spectra (Yi & Boughn 1998). Since X-ray and radio emission occurs in the same plasma, the X-ray and radio luminosities are correlated and can be used to estimate the mass of the central black hole (Yi & Boughn 1998).

Radio jets are observed to be widespread in early-type radio galaxies (e.g., Rees et al. 1982). On the other hand, ADAFs have been shown to have positive net energy near the rotational axis (Narayan & Yi 1995a) and, therefore, are particularly susceptible to outflows. If X-ray emission from XBGNs is due to ADAFs, it is plausible that radio jets would also be present and could dominate the total radio luminosities of these sources. In fact, Falcke, Wilson, & Ho (1999) recently argued that a large fraction of relatively radio-dim active galaxies, QSOs, and LINERs possess parsec-scale radio jets. If so, it might be the case that the radio luminosities of nearly all XBGNs are dominated by jet emission. Nevertheless, high angular resolution observations could still reveal the presence of an ADAF radio core with its characteristic inverted spectrum. Many of the sources (XBGNs and Seyfert galaxies) listed below are jet-dominated sources and, yet, have 15 GHz core luminosities similar to those predicted by the ADAF model.

Franceschini, Vercellone, & Fabian (1998) reported an intriguing correlation between the total radio luminosities and the dynamically determined black hole masses of a small sample of XBGNs consisting primarily of early-type galaxies. They interpreted the correlation as due to ADAF radio emission around massive black holes accreting from the hot gas readily available in early-type galactic nuclei. Although their explanation (assuming the accretion rate is determined by the Bondi rate and the gas density is directly related to the black hole mass) is largely implausible (see § 3), the correlation does suggest an interesting trend in radio properties. Many of their sources are likely to contain radio jets. By combining them with those used in Yi & Boughn (1998), we attempt to distinguish radio-jet from pure ADAF emission in XBGNs. We examine possible radio/X-ray luminosity relations in pure ADAF flows and in radio-jet sources with known black hole masses. Particular attention

¹ Institute for Advanced Study, Olden Lane, Princeton, NJ 08540; yi@sns.ias.edu; also at Center for High Energy Astrophysics and Isotope Studies, Research Institute for Basic Sciences and Department of Physics, Ewha University, Seoul, Korea.

² Department of Astronomy, Haverford College, Haverford, PA 19041; sboughn@haverford.edu.

is paid to the origin of radio activity, and we suggest that among XBGs it is useful to designate two populations, radio-bright and radio-dim, which are analogous to more powerful AGN populations.

We designate as “radio dim” those sources with 5 GHz luminosities of $\nu L_\nu \lesssim 10^{38}$ ergs s^{-1} . Even if jets are present in these sources, they are likely to be relatively weak, parsec-scale jets and may still appear as core-dominated sources when observed with moderate angular resolution. The jet emission in such sources has a flat or inverted spectrum (e.g., Falck et al. 1999). XBGs with luminosities $L_R \gtrsim 10^{38}$ ergs s^{-1} are designated as “radio bright” (to distinguish them from the conventional “radio loud” sources, which are much more powerful). Such sources have more substantial jets and will, therefore, invariably appear extended as well as exhibit steeper spectra.

2. RADIO/X-RAY EMISSION FROM ACCRETING MASSIVE BLACK HOLES

2.1. Emission from Optically Thin ADAFs

In high-temperature, optically thin ADAFs, the hard X-ray emission results from bremsstrahlung and Comptonization (Narayan & Yi 1995b; Rees et al. 1982). The Compton-upscattered soft photons are generated by synchrotron emission, which is subject to self-absorption. Assuming an equipartition-strength magnetic field, all of the relevant emission components from radio to X-ray are explicitly calculable in terms of black hole mass M_{bh} , mass accretion rate \dot{M} , and the viscosity parameter α , for which we adopt the value 0.3 (Frank et al. 1992).

In ADAFs, radio emission arises directly from synchrotron emission with magnetic field $B \sim 1.1 \times 10^4 m_7^{-1/2} \dot{m}_{-3}^{1/2} r^{-5/4}$ G, where $m = M_{\text{bh}}/M_\odot$, $m_7 = m/10^7$, $\dot{m} = \dot{M}/\dot{M}_{\text{Edd}}$, $\dot{m}_{-3} = \dot{m}/10^{-3}$, and $r = R/R_s$ with $\dot{M}_{\text{Edd}} = 1.39 \times 10^{25} m_7$ g s^{-1} , and $R_s = 2.95 \times 10^{12} m_7$ cm. The optically thin synchrotron emission is self-absorbed up to a frequency $\nu_{\text{syn}}(r) \sim 9 \times 10^{11} m_7^{-1/2} \dot{m}_{-3}^{1/2} T_{e9}^2 r^{-5/4}$ Hz, where $T_{e9} = T_e/10^9$ K is the electron temperature. At radio frequencies, the luminosity is given by (e.g., Yi & Boughn 1998, and references therein)

$$L_{R,\text{adv}}(\nu) = \nu L_\nu^{\text{syn}} \sim 2 \times 10^{32} x_{M3}^{8/5} m_7^{6/5} \dot{m}_{-3}^{4/5} T_{e9}^{21/5} \nu_{10}^{7/5} \text{ ergs } s^{-1}, \quad (1)$$

where $\nu_{10} = \nu/10^{10}$ Hz and $x_{M3} = x_M/10^3$ is the dimensionless synchrotron self-absorption coefficient (Narayan & Yi 1995b). Since $x_{M3} \propto (m\dot{m})^{1/4}$ and $T_{e9} \lesssim 10$ is only weakly dependent on m and \dot{m} (e.g., Mahadevan 1996), we obtain the approximate relation (for $\nu = 15$ GHz)

$$L_{R,\text{adv}} \sim 3 \times 10^{36} m_7^{8/5} \dot{m}_{-3}^{6/5} \text{ ergs } s^{-1}. \quad (2)$$

The 2–10 keV X-ray emission from ADAFs is due to bremsstrahlung and Comptonization of synchrotron photons. At low mass accretion rates, $\dot{m} \lesssim 10^{-3}$, the X-ray luminosity has a significant bremsstrahlung contribution, whereas at relatively high mass accretion rates, $10^{-3} \lesssim \dot{m} \lesssim 10^{-1.6}$, Comptonization dominates in the 2–10 keV band. ADAFs can only exist for mass accretion rates below a critical value, $\dot{m} < \dot{m}_{\text{crit}} \approx 10^{-1.6}$ (Rees et al. 1982; Narayan & Yi 1995b). Yi & Boughn (1998) have shown that the 2–10 keV X-ray luminosity is related to the 15 GHz radio luminosity by a simple relation:

$$L_{R,\text{adv}} \sim 1 \times 10^{36} m_7 (L_{X,\text{adv}}/10^{40} \text{ ergs } s^{-1})^y, \quad (3)$$

where $y \sim 1/5$ for systems with $\dot{m} < 10^{-3}$ and $y \sim 1/10$ for systems with $\dot{m} > 10^{-3}$. For our discussions, we adopt $y = 1/7$, which is a reasonably good approximation for $10^{-4} \lesssim \dot{m} \lesssim 10^{-1.6}$. The bolometric luminosity, which is dominated by the X-ray luminosity for $\dot{m} \gtrsim 10^{-3}$, is roughly given by $L_{\text{adv}} \sim 30 \dot{m}^2 L_{\text{Edd}}$, where $L_{\text{Edd}} = 0.1 \dot{M}_{\text{Edd}} c^2$ (e.g., Yi 1996).

2.2. Emission from Optically Thick Disks

In ADAFs, optical/UV emission is characteristically weak, which distinguishes ADAFs from the high radiative efficiency accretion disks commonly assumed for luminous AGNs. For the high accretion rates required by luminous AGNs, i.e., $\dot{m} \gtrsim 10^{-1.6}$, ADAFs do not exist (Narayan & Yi 1995b; Rees et al. 1982). It is widely assumed that at such high rates, accretion takes the form of a geometrically thin, optically thick accretion flow with a hot, X-ray-emitting corona (Frank et al. 1992). Then

$$L_{X,\text{disk}} \sim \eta_{\text{eff}} \dot{M} c^2 \sim 1.3 \times 10^{42} (\eta_{\text{eff}}/0.1) m_7 \dot{m}_{-3} \text{ ergs } s^{-1}, \quad (4)$$

where η_{eff} is the radiative efficiency of the accretion flow. The efficiency must be high, $\eta_{\text{eff}} \sim 0.1$, to account for the observed X-ray luminosities.

2.3. Radio-Jet Power

Most AGNs have radio luminosities that far exceed those predicted by the ADAF model (see, for example, Fig. 1). That there exists a wide range of radio luminosities for a relatively narrow X-ray luminosity range (of X-ray-selected

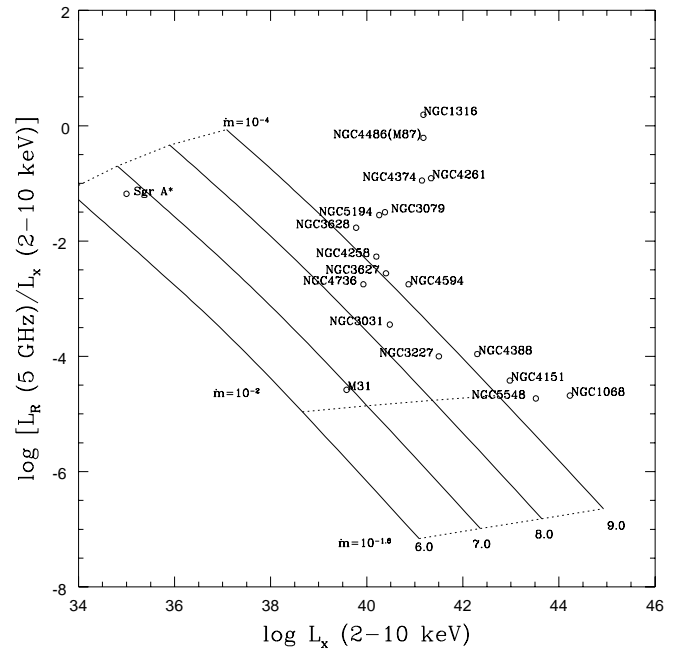


FIG. 1.—Ratio of 5 GHz radio luminosity L_R to 2–10 keV X-ray luminosity L_X vs. L_X for XBGs. The radio luminosities include both core and extended contributions. Scaling from other frequencies is discussed in the text. The sources are adopted from Yi & Boughn (1998) and Franceschini et al. (1998). The solid lines are the ADAF predictions for black hole masses of 10^6 – $10^9 M_\odot$ (marked by log values at the bottom of each curve). For each line, the dimensionless mass accretion rate \dot{m} varies from 10^{-4} (upper dotted line) to $10^{-1.6}$ (lower dotted line), the maximum allowed ADAF accretion rate (as in Yi & Boughn 1998).

sources) is likely the result of radio jets of various strengths; however, it is still unclear just how radio-emitting jets are powered.

Given the fact that ADAFs are prone to outflows/jets (Narayan & Yi 1995a; Rees et al. 1982), it is likely that many ADAF sources have radio jets. Neither the ADAFs nor the thin disk models can self-consistently account for this radio emission. However, if the radio jet is powered by a rotating black hole accreting from a magnetized plasma, as is generally believed, the radio power can be described by the Blandford-Znajek process (e.g., Frank et al. 1992), according to which $L_{R,jet} \propto \bar{a}^2 M_{bh}^2 B^2$ or

$$L_{R,jet} \sim 1.2 \times 10^{42} \bar{a}^2 \epsilon_{jet} m_7 \dot{m}_{-3}, \quad (5)$$

where $\bar{a} \leq 1$ is the black hole spin parameter and $\epsilon_{jet} \leq 1$ is the efficiency of the radio emission.

3. RADIO/X-RAY LUMINOSITY RELATION AND BLACK HOLE MASSES

Figure 1 is a plot of the ratio of the 5 GHz total (as opposed to “core”) radio luminosity to 2–10 keV X-ray luminosity versus X-ray luminosity for a collection of LINERs, moderate- to low-luminosity Seyfert galaxies, X-ray-bright elliptical galaxies, and the weak nuclear sources Sgr A* and M31. The sources were compiled from Yi & Boughn (1998) and Franceschini et al. (1998). X-ray fluxes were converted to 2–10 keV fluxes in those cases in which the data were in a different band, and they are uncertain by a factor of a few at most. The 5 GHz radio fluxes are from the Green Bank survey (Becker, White, & Edward 1991; Gregory & Condon 1991). The solid lines are predicted for ADAFs of different black hole masses and are discussed in more detail below and in Yi & Boughn (1998).

Dynamical black hole mass estimates are available for NGC 1068, NGC 1316, NGC 4258, NGC 4261, NGC 4374, NGC 4486, NGC 4594, M31, and Sgr A*. The mass of NGC 1068 is from Greenhill et al. (1996); that of NGC 4258 is from Herrnstein et al. (1998); that of Sgr A* is from Eckart & Genzel (1997); those of M31, M87, and NGC 4594 are from Richstone et al. (1998); that of NGC 4261 is from Richstone et al. (1998) and Ferrarese, Ford, & Jaffe (1996); and those of NGC 1316 and NGC 4374 are from Franceschini et al. (1998). Uncertainties in these masses are not easily quantified; however, from the spread of different mass estimates, it seems likely that they are accurate to within a factor of 2. Figure 2 depicts the correlation of 5 GHz radio luminosity and black hole mass that was noted by Franceschini et al. (1998). They also noted that the correlation of X-ray luminosity and black hole mass is very weak (see Fig. 3).

Franceschini et al. (1998) argue that ADAF radio emission is responsible for the correlation between radio luminosity and black hole mass. They assume that the density of the accreted matter at large distances from the black hole is proportional to the black hole mass, i.e., $\rho_\infty \propto M_{bh}$, and that $M_{bh} \propto M_{gal} \propto c_{s,\infty}^4$, where $c_{s,\infty}$ is the sound speed of the accreting gas. The latter relation is adopted from the Faber-Jackson relation. Assuming Bondi accretion, then $\dot{M} \propto M_{bh}^2 \rho_\infty / c_s^3 \propto M_{bh}^{9/4}$. If one ignores the dependence of x_{M3} on \dot{M} , equation (1) implies that $L_{R,adv} \propto M_{bh}^{11/5}$. This is the power-law mass-luminosity relation derived by Franceschini et al. (1998) (dashed line, Fig. 2). The power law appears to agree with the trend in the data, although its statistical significance is obviously limited due to the sample

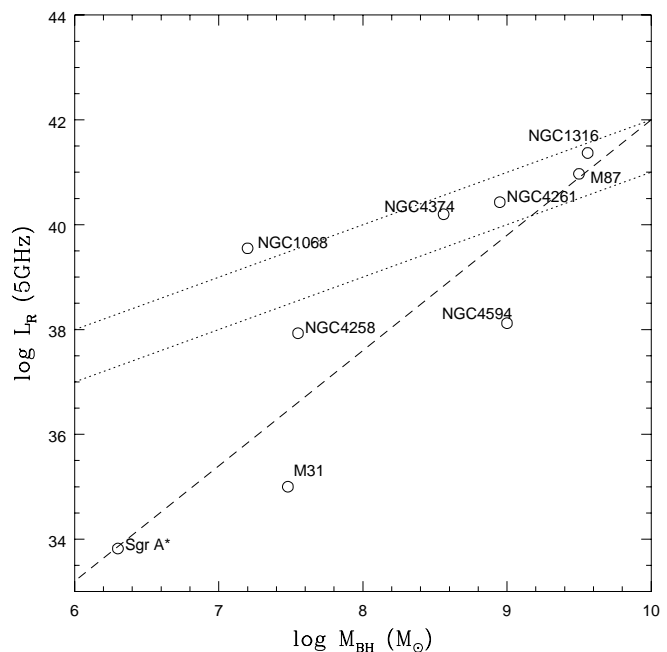


FIG. 2.—The 5 GHz L_R vs. M_{bh} for the nine sources with black hole mass estimates. The radio fluxes are as in Fig. 1. The dashed line is the $L_R \propto M_{bh}^{11/5}$ relation suggested in Franceschini et al. (1998). The two dotted lines depict the $L_R \propto \bar{a}^2 M_{bh}$ relation expected for radio-jet sources with a spread of a factor ~ 10 in \bar{a}^2 (see text). The references for the dynamical mass estimates are listed in the text.

size and uncertainties in the radio fluxes (if one includes the dependence of x_{M3} on \dot{M} , then the power-law slope is changed somewhat, but the following conclusions are the same).

However, such an explanation inevitably predicts a strong correlation between L_X and M_{bh} . For ADAFs,

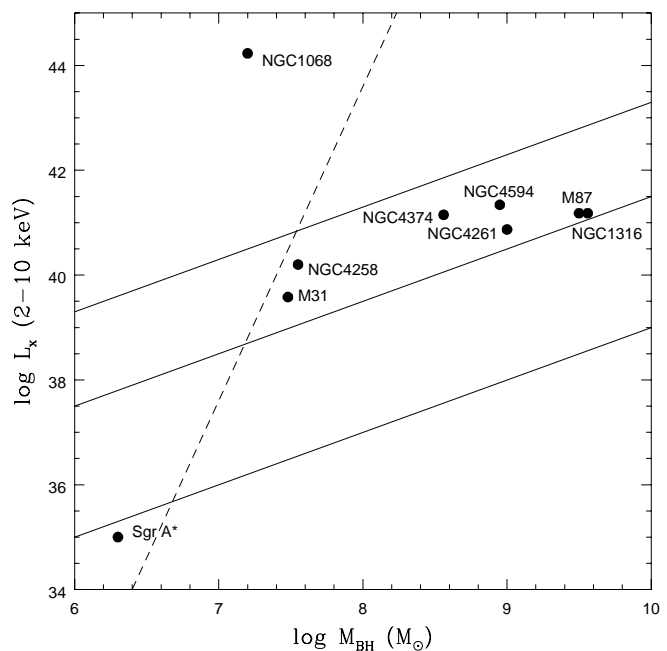


FIG. 3.—The 2–10 keV L_X vs. M_{bh} for the same sources as in Fig. 2. The dashed line is the steep correlation $L_X \propto M_{bh}^6$ expected if the Franceschini et al. (1998) model were valid. The three solid lines correspond to $L_X \propto M_{bh}$ correlations for $\dot{m} \sim 10^{-2}$, 10^{-3} , and 10^{-4} from top to bottom (see text). The references for the dynamical mass estimates are listed in the text.

$L_{X,adv} \propto m\dot{m}^x$, where $x = 2$ if X-rays come from bremsstrahlung and $x > 2$ if X-rays are from multiple Compton scattering (Yi & Boughn 1998; Yi 1996). Therefore, $L_{X,adv} \propto M_{bh}^{(5x+4)/4}$ and $L_{R,adv}/L_{X,adv} \propto L_{X,adv}^{(24-25x)/(20+25x)}$. For a wide range of x , $2 \leq x \leq 10$, we expect $L_{R,adv}/L_{X,adv} \propto L_{X,adv}^{-0.4}$ to $L_{X,adv}^{-0.8}$. Therefore, all sources shown in Franceschini et al. (1998) should fall in a single band with a slope of ~ -0.6 in the L_R/L_X versus L_X plane. This is not evident in Figure 1. The predicted X-ray mass-luminosity relation is quite steep, $L_{X,adv} \propto M_{bh}^\beta$, with $3.5 \leq \beta \leq 13.5$ for $2 \leq x \leq 10$, and is not consistent with observations as indicated in Figure 3, where the dashed line is for $x = 4$, i.e., $\beta = 6$. Apparently, the most massive black hole sources are too X-ray dim to be compatible with the Franceschini et al. (1998) model. If the measured radio luminosities are indeed from ADAFs, the observed black hole masses predict much higher L_X than observed. Therefore, the correlation found by Franceschini et al. (1998) cannot be attributed to ADAFs powered by Bondi accretion. An alternative explanation is that the observed radio luminosities are due to much more energetic sources, e.g., jets, whose luminosities are not directly related to the radio luminosity of the ADAF core.

If the excess radio emission is due to jet activity, then equation (5) and $L_{X,adv} \propto m\dot{m}^x$ imply

$$L_{R,jet} \propto \bar{a}^2 L_{X,adv}^{1/x} M_{bh}^{(x-1)/x}, \quad (6)$$

and for a wide range of $x \geq 4$, we expect the dominant scaling $L_{R,jet} \propto \bar{a}^2 M_{bh}$. Then, the observed L_R versus M_{bh} plot in Figure 2 could simply be a result of the combination of $L_R \propto M_{bh}$ and a distribution of \bar{a} 's (dotted lines). If the accretion rate is controlled by the Bondi rate, i.e., $\dot{M} \propto M_{bh}^{9/4}$, then $L_X \propto M_{bh}^{(5x+4)/4}$ and $L_{R,jet} \propto \bar{a}^2 M_{bh}^{9/4}$, which is similar to the $L_{R,adv} \propto M_{bh}^{11/5}$ relation of Franceschini et al. (1998).

The radio and X-ray emission from an ADAF are given by $L_{X,adv} \propto m\dot{m}^x$, $L_{R,adv} \propto M_{bh}^{8/5} \dot{m}^{6/5}$ (eq. [2]), and, therefore, $L_{R,adv} \propto m^{(8x-6)/5x} L_{X,adv}^{6/5x}$ (Yi & Boughn 1998). These trends are shown as solid lines in Figures 1 and 3. In Figure 3, the X-ray emission for most of the sources is well accounted for if \dot{m} varies from 10^{-2} to 10^{-3} . Since ADAF radio emission is highly localized ($\ll 1$ pc), it is not surprising that the total radio fluxes plotted in Figure 1 exceed those predicted by ADAFs. Figures 4 and 5 are plots of the 15 GHz core luminosities of these same sources. In a few cases, radio fluxes were converted from 5 to 15 GHz using the $\nu^{7/5}$ power-law of equation (1). While this conversion is inappropriate for steep-spectrum sources, it allows a direct comparison of these luminosities with those predicted for an ADAF. In any case, such values are in error by at most a factor of a few (if a source has a steep spectrum, i.e., $\nu L_\nu \propto \nu^{0.2}$, the error is less than a factor of 4). The solid lines in Figures 4 and 5 are the same as those in Figures 3 and 1 and they are, indeed, compatible with most of the sources; however, only in three cases is the angular resolution good enough to approximately resolve the ADAF core. The sources are discussed individually in § 4.

The ratio of jet to ADAF radio emission depends only weakly on black hole mass and accretion rate. From equations (2) and (5),

$$L_{R,jet}/L_{R,adv} \sim 4 \times 10^5 \bar{a}^2 \epsilon_{jet} m_7^{-1/5} \dot{m}_{-3}^{1/5}, \quad (7)$$

i.e., $L_{R,jet}$ can far exceed $L_{R,adv}$ for sources with typical M_{bh} and \dot{M} unless $\bar{a} \ll 2 \times 10^{-3} \epsilon_{jet}^{-1/2}$. This appears to be the case for many of the sources in Figure 1.

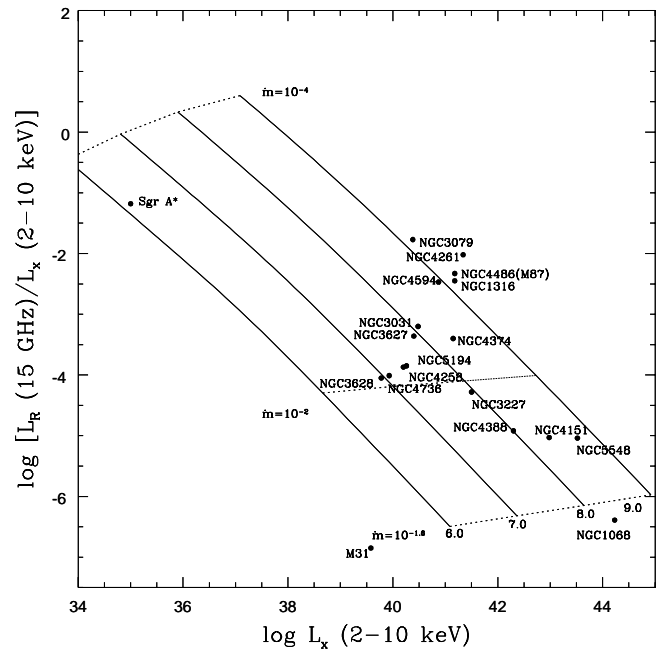


FIG. 4.—Ratio of 15 GHz core radio luminosity L_R to 2–10 keV X-ray luminosity L_X vs. L_X for the sources in Fig. 1. The solid and dotted lines are the same ADAF predictions as in Fig. 1. Note: $\dot{m} \sim 10^{-1.6}$ is the maximum allowed ADAF accretion rate.

If L_X is from a thin disk and L_R is from a jet (since a thin disk itself is unable to emit in the radio), we expect (from eqs. [4] and [5])

$$L_{R,jet}/L_{X,disk} \sim \bar{a}^2 \epsilon_{jet}/\eta_{eff} \leq \epsilon_{jet}/\eta_{eff}. \quad (8)$$

For radio-bright galaxies with $\bar{a} \sim 1$, this ratio is independent of X-ray luminosity or black hole mass. For radio-dim sources (e.g., $\bar{a} \ll 1$), we expect $L_X \gg L_R$.

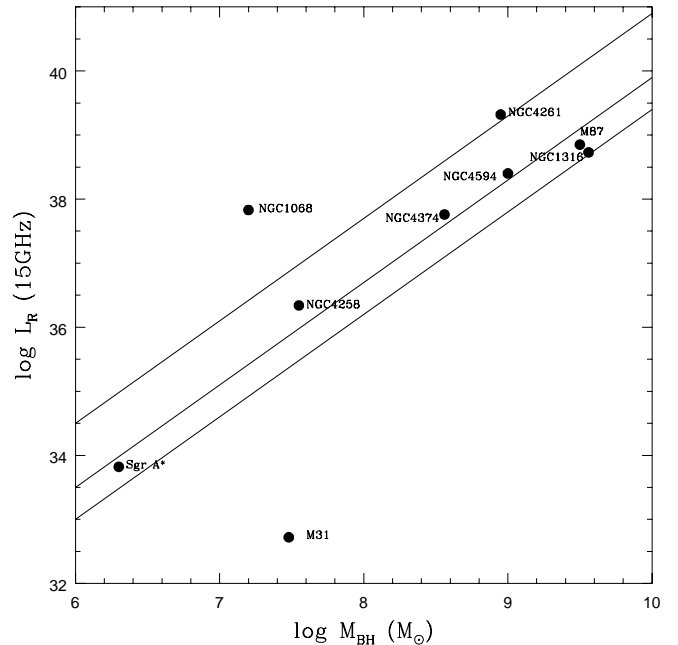


FIG. 5.—The 15 GHz core radio luminosity vs. M_{bh} for the nine sources in Fig. 2. The three solid lines correspond to the ADAF-based relation $L_R \propto \dot{m}^{6/5} M_{bh}^{8/5}$ for the three \dot{m} values shown in Fig. 3. The references for the dynamical mass estimates are listed in the text.

4. DISCUSSION OF INDIVIDUAL SOURCES

4.1. M87, NGC 4258, and Sgr A*

These three sources have estimated black hole masses and, in addition, have been the subject of high angular resolution radio observations (VLBI, VLBA, and VLA, respectively). While M87 and NGC 4258 have relatively strong, extended radio emission from jets, the high spatial resolution ($\ll 1$ pc) of the radio observations affords a nearly resolved view of the hypothetical core ADAF. The masses implied by their locations on Figure 4 are within a factor of 2 of the dynamical estimates for these two sources.

All three of these sources have been previously identified as ADAF candidates (Reynolds et al. 1996; Lasota et al. 1996; Narayan, Yi, & Mahadevan 1995). However, Herrnstein et al. (1998) have argued that the NGC 4258 core source used in this paper is actually one of two unresolved radio jets located ~ 0.01 pc from the warped plane of the accretion disk. If future observations strengthen this conclusion, then the ADAF mechanism for NGC 4258 will be called into question (see Blackman 1998).

Sgr A* is distinct from the other sources discussed in this paper in that it has a much smaller X-ray luminosity due presumably to a low accretion rate. Nevertheless, Narayan et al. (1995) have modeled it as an ADAF, so we include it here as an example of a low-mass, low accretion rate ADAF. We have plotted in Figures 1, 3, and 4 the *ROSAT* X-ray flux corrected for extinction (Prehehl & Trumper 1994). The uncertainty in the extinction-corrected X-ray flux has little consequence since for a given core radio flux, the X-ray flux is nearly independent of black hole mass. The location of the Sgr A* point would simply be translated along a line that is nearly parallel to the theoretical curves in Figures 1 and 4.

4.2. NGC 1068, NGC 1316, NGC 4261, NGC 4374, NGC 4594, and M31

These are the remaining sources for which there are dynamical estimates of the masses of the central black holes, although none has been observed in the radio with very high angular resolution. NGC 4594 (M104) is a radio-dim, flat-spectrum source with no sign of jet activity. VLA observations (Hummel, van der Hulst, & Dickey 1984) indicate a core-dominated source with a size less than 1 pc. If this radio source is interpreted as an ADAF, then the black hole mass implied by Figure 4 is the same as the dynamical estimate. NGC 1316, NGC 4261, and NGC 4374, on the other hand, are radio-bright sources (see Fig. 1). NGC 1316 is a bright, lobe-dominated radio galaxy. Because of relatively poor angular resolution, its core flux is not well defined; however, the radio luminosity within $3''$ – $5''$ is within a factor of 2 of that predicted for an ADAF flow with the measured black hole mass. NGC 4261 and NGC 4374 are also extended sources but again with core luminosities comparable (within a factor ~ 2) to that predicted by the ADAF model. Considering the uncertainties of the X-ray and radio observations and of the dynamical mass estimates, the level of agreement is impressive.

It is clear from Figure 4 that NGC 1068 and M31 do not fit the ADAF model; however, both are unusual sources. The direct X-rays from the nucleus of NGC 1068 appear to be highly absorbed with the observed X-ray flux consisting entirely of scattered photons. The inferred intrinsic X-ray luminosity is likely to be $L_X \gtrsim 5 \times 10^{43}$ ergs s^{-1} (e.g.,

Koyama et al. 1989). The Eddington luminosity for the estimated black hole mass $M_{bh} \sim 2 \times 10^7 M_\odot$ is $L_{Edd} \sim 2 \times 10^{45}$ ergs s^{-1} ; therefore, $L_X \gtrsim 3 \times 10^{-2} L_{Edd}$. This implies a bolometric luminosity in excess of the maximum allowed for ADAF flows (Narayan, Mahadevan, & Quataert 1999), so it is unlikely that the X-ray emission is from an ADAF. NGC 1068 has a resolved central core with an observed 15 GHz luminosity of $\sim 7 \times 10^{37}$ ergs s^{-1} (Sadler et al. 1995) together with clear jet structures. If the X-ray emission occurs with high efficiency, $\sim 10\%$, the observed L_X implies $\dot{m} \sim 2 \times 10^{-2}$. In this case, $L_{R,jet} \leq 5 \times 10^{43} \bar{a}^2 \epsilon_{jet}$, which is far more than the observed L_R even with $\epsilon_{jet} \ll 1$ for $\bar{a} \sim 1$. Therefore, NGC 1068 is likely to be a typical radio-quiet, luminous Seyfert galaxy (Falcke et al. 1999).

M31 has an extremely low core radio luminosity, 5×10^{32} ergs s^{-1} (Gregory & Condon 1991). If this is attributed to an ADAF with $M_{bh} = 3 \times 10^7 M_\odot$, then the implied accretion rate is very small, $\dot{m} \sim 10^{-6}$, and the expected ADAF X-ray luminosity is $L_X \sim 4 \times 10^{34}$ ergs s^{-1} , much less than that observed. In this case it is possible that the observed L_X is dominated by a few bright X-ray binaries similar to those recently reported in M32 (Loewenstein et al. 1998). Indeed, Sgr A* is surrounded by bright, resolved X-ray sources (e.g., Genzel, Hollenbach, & Townes 1994) and if put at the distance of M31 would appear as a brighter, unresolved core. Finally, it is not at all clear whether the two-temperature ADAF model is valid at such low accretion rates.

4.3. NGC 3031, NGC 3079, NGC 3627, NGC 3628, NGC 4736, and NGC 5194

These sources are all nearby LINERs with similar 2–10 keV X-ray luminosities, $6 \times 10^{39} < L_X < 3 \times 10^{40}$. There are no dynamical mass estimates for the black holes in any of them. It is interesting to note, however, that with the exception of NGC 3079 the core radio luminosities are consistent with those predicted by ADAFs for black hole masses of $\sim 10^7$ to $\sim 10^8 M_\odot$ (see Fig. 4). The larger luminosity of NGC 3079 would require $M_{bh} = 1.4 \times 10^9 M_\odot$. In addition, all of the sources have either flat or inverted radio spectra.

None of these is a particularly strong radio source; however, only one of them, NGC 3031, is dominated by core emission. Coincidentally, this is the only source for which there are high angular resolution (VLBI) radio observations (Bietenholz et al. 1996; Reuter & Lesch 1996; Turner & Ho 1994). The spectrum is inverted ($\propto \nu^{1/3}$) up to 100 GHz, where it begins to turn over. This is consistent with an ADAF. At 22 GHz the core is barely resolved, ~ 0.1 mas, which implies a linear size of ~ 0.002 pc. This is also consistent with an ADAF. If the radio and X-ray luminosities are, indeed, due to an ADAF, then the implied black hole mass is $\sim 1 \times 10^8 M_\odot$. It will be interesting to see if future dynamical analyses confirm this value.

4.4. NGC 3227, NGC 4151, NGC 5548, and NGC 4388

These four sources are all classified as Seyfert galaxies, and none is a particularly strong radio source (see Fig. 1). Their radio and X-ray luminosities are consistent with ADAFs onto $(1\text{--}5) \times 10^8 M_\odot$ black holes and with accretion rates below the critical value (Fig. 4). Because the ADAF cores are unresolved, it is certainly possible that the radio core luminosities and hence masses are both overesti-

mates. However, it seems unlikely that such corrections would result in moving these sources from the ADAF region.

These four sources are on average ~ 600 times more X-ray luminous than the six LINERs discussed above but have only twice the core radio luminosity (see Fig. 4). There are no black hole mass estimates for any of these sources, so it is not possible to make quantitative comparisons of their emissions with those predicted by the ADAF model. However, to the extent that the average black hole masses of these sources are comparable, we note that the narrow range of core radio luminosity is qualitatively consistent with the weak dependence of L_R on L_X (see eq. [3]). The wide range in X-ray luminosities is then presumably due to differences in the accretion rates for these sources.

It should be emphasized that there is considerable uncertainty in the above comparisons of dynamical mass estimates with ADAF predictions. In addition to the observational and modeling uncertainties, one must contend with the intrinsic variability of ADAF sources (Blackman 1998; Ptak et al. 1998). Multiple-epoch radio and X-ray observations are necessary to quantify the extent of the variability and to estimate the mean fluxes. For these reasons, the good agreement between the mass estimates and ADAF predictions in this paper may be partly fortuitous.

5. CLASSIFICATION OF X-RAY-BRIGHT GALACTIC NUCLEI

The previous discussion suggests a useful classification scheme based on the radio and X-ray luminosities of XBGNs and moderate-luminosity Seyfert galaxies. From Figures 1 and 6 it is clear that the 5 GHz ADAF (total) radio luminosity is $L_R \lesssim 10^{38}$ ergs s^{-1} unless $M_{bh} \gtrsim 10^9 M_\odot$

M_\odot and the accretion rate is near the maximum allowed by ADAFs. Therefore, we designate a source as radio bright if its total (core plus jet) 5 GHz radio luminosity satisfies $L_R > 10^{38}$ ergs s^{-1} . Note that this does not preclude XBGNs with luminosities below this value from being jet dominated; in fact, of the sources in Figure 1, only NGC 3031 and NGC 4594 are ADAF core dominated. However, XBGNs designated as radio bright will certainly be jet-dominated radio sources. Figure 6 illustrates this classification for the same sources as in Figure 1. The upper dashed curve corresponds to the ADAF luminosity for a $10^9 M_\odot$ black hole (which is motivated by the fact that black holes with $M_{bh} > 10^9 M_\odot$ are rare), and the lower dashed curve corresponds to maximally accreting ADAFs, i.e., $\dot{m} = 10^{-1.6}$. Sources falling within the region at the bottom left of the diagram (bounded by the dashed curves) are designated radio-dim XBGNs. As noted, these are presumably ADAFs with little to moderate jet activity. Sources to the left in this region have low accretion rates, while sources at the bottom have low-mass central black holes. Above this region are the radio-bright XBGNs discussed above. Sources at the right of the diagram are too X-ray bright to be the result of an ADAF, but rather require the high efficiency accretion mechanism of powerful AGNs. These classifications are not unambiguous. For example, an AGN with a low-mass central black hole and low X-ray luminosity but with moderate jet activity could appear in the upper left part of the radio-dim XBGN region, even though the radio luminosity far exceeds that predicted by the ADAF mechanism. High angular resolution radio observations, an estimate of black hole mass, and/or the determination of the radio spectral index would likely distinguish between these two cases.

6. CONCLUSIONS

For a given black hole mass, the ADAF model predicts a unique radio/X-ray luminosity relation. ADAF radio emission is essentially characterized by an inverted spectrum and a very compact emission region, $\ll 1$ pc. So far, the only sources for which there are both high angular resolution radio data and dynamical estimates are M87, NGC 4258, and Sgr A*. The observations for all three are consistent with the predictions of the ADAF emission model. There are four other sources (NGC 1316, NGC 4261, NGC 4374, and NGC 4594) for which moderate angular resolution radio observation and dynamical black hole mass estimates are available. The X-ray and core radio luminosities of these XBGNs are also consistent with the ADAF model. Considering observational and modeling uncertainties, the agreement is quite good.

In the future, high angular resolution radio observations combined with X-ray observations might enable the central black hole masses of XBGNs to be estimated. For example, the nuclear source in NGC 3031 (M81) is both small (~ 0.002 pc) and has an inverted spectrum (Reuter & Lesch 1996). Based on its X-ray and core radio flux, the ADAF implies a black hole mass of $M_{bh} \sim 1 \times 10^8 M_\odot$ (see Fig. 4). Although source variability has not yet been taken into account, we suggest that future dynamical estimates of the central black hole of NGC 3031 will not be far from this value.

Multiple-epoch, high angular resolution, high-frequency radio observations will be crucial to test the ADAF

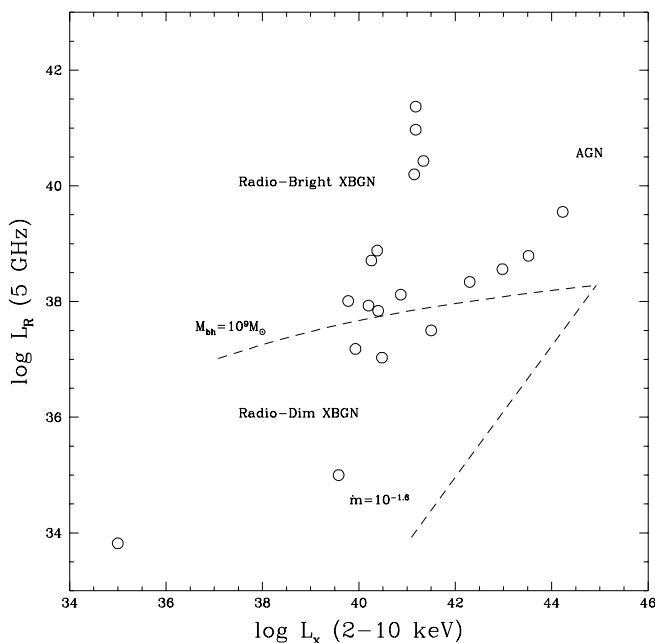


FIG. 6.—Schematic classification of XBGN sources according to 5 GHz total radio and 2–10 keV X-ray luminosities. The sources are the same as in Fig. 1. The upper dashed line corresponds to the ADAF L_R for $M_{bh} = 10^9 M_\odot$, and the lower dashed line corresponds to the maximum ADAF accretion rate, $\dot{m} = 10^{-1.6}$. The region on the right is occupied by powerful AGNs in which the ADAF mechanism cannot be operating.

mechanism and, subsequently, to estimate central black hole masses. Even with such observations, it will still be difficult to characterize sources if they are strongly obscured as expected in Seyfert 2's. Relatively low X-ray luminosity sources will be detected by *AXAF* and will greatly improve the test of the ADAF paradigm among LINERs and other relatively low-luminosity XBGs with $L_X \lesssim 10^{40}$ ergs s⁻¹.

The compact, inverted-spectrum characteristics of ADAFs can also be used to distinguish them from small-scale jets, which are abundant in XBGs. A moderate excess of radio emission from such a source probably indicates the presence of low-level (parsec-scale) jet activity. We propose an XBG classification scheme analogous to the radio-loud/radio-quiet classification of powerful AGNs. Whereas it is likely that the radio luminosities for all powerful AGNs (radio quiet and radio loud) are due to jets, it is

possible for some radio-dim XBGs to be dominated by an ADAF core. On the other hand, radio-bright XBGs are undoubtedly jet dominated. ADAFs are strong, hard X-ray sources, and to the extent that they are present in XBGs, it is likely that the 2–10 keV core luminosities of XBGs will be dominated by ADAF emission.

We would like to thank R. van der Marel and Douglas Richstone for useful information on black hole masses, Pawan Kumar and Tal Alexander for help with NGC 1068, and Ramesh Narayan for early discussions on spectral states of accreting massive black holes. This work was supported in part by the SUAM Foundation and the Korea Research Foundation (1998-001-D00365) (I. Y.) and NASA grant NAG5-3015 (S. P. B.).

REFERENCES

- Becker, R. H., White, R. L., & Edward, A. L. 1991, *ApJS*, 75, 1
 Bietenholz, M. F., et al. 1996, *ApJ*, 457, 604
 Blackman, E. G. 1998, *MNRAS*, 299, L48
 Di Matteo, T., & Fabian, A. C. 1997, *MNRAS*, 286, 393
 Eckart, A., & Genzel, R. 1997, *MNRAS*, 284, 576
 Fabian, A. C., & Rees, M. J. 1995, *MNRAS*, 277, L55
 Falcke, H., Wilson, A. S., & Ho, L. C. 1997, in *Relativistic Jets in AGNs*, ed. M. Ostrowski, M. Sikora, G. Madejski, & M. Begelman (Kraków: Uniwersytet Jagiellonski), 13
 Ferrarese, L., Ford, H. C., & Jaffe, W. 1996, *ApJ*, 470, 444
 Franceschini, A., Vercellone, S., & Fabian, A. C. 1998, *MNRAS*, 297, 817
 Frank, J., King, A. R., & Raine, D. 1992, *Accretion Power in Astrophysics* (Cambridge: Cambridge Univ. Press)
 Genzel, R., Hollenbach, D., & Townes, C. H. 1994, *Rep. Prog. Phys.*, 57, 417
 Greenhill, L. J., Gwinn, C. R., Antonucci, R., & Barvainis, R. 1996, *ApJ*, 472, L21
 Gregory, P. D., & Condon, J. J. 1991, *ApJS*, 75, 1011
 Herrnstein, J. R., Greenhill, L. J., Moran, J. M., Diamond, P. J., Inoue, M., Nakai, N., & Miyoshi, M. 1998, *ApJ*, 497, L69
 Hummel, E., van der Hulst, J. M., & Dickey, J. M. 1984, *A&A*, 134, 207
 Koyama, K., et al. 1989, *PASJ*, 41, 731
 Lasota, J.-P., Abramowicz, M. A., Chen, X., Krolik, J., Narayan, R., & Yi, I. 1996, *ApJ*, 462, 142
 Loewenstein, M., Hayashida, K., Toneri, T., & Davis, D. S. 1998, *ApJ*, 497, 681
 Mahadevan, R. 1996, *ApJ*, 465, 327
 Narayan, R., Mahadevan, R., & Quataert, E. 1999, in *The Theory of Black Hole Accretion Disks*, ed. M. A. Abramowicz, G. Bjornsson, & J. E. Pringle (Cambridge: Cambridge Univ. Press), in press
 Narayan, R., & Yi, I. 1995a, *ApJ*, 444, 231
 ———. 1995b, *ApJ*, 452, 710
 Narayan, R., Yi, I., & Mahadevan, R. 1995, *Nature*, 374, 623
 Osterbrock, D. E. 1989, *Astrophysics of Gaseous Nebulae and Active Galactic Nuclei* (Mill Valley: University Science Books)
 Predehl, P., & Trumper, J. 1994, *A&A* 290, L29
 Ptak, A., Yaqoob, T., Mushotzky, R., Serlemitsos, P., & Griffith, R. 1998, *ApJ*, 501, L37
 Rees, M. J., Begelman, M. C., Blandford, R. D., & Phinney, E. S. 1982, *Nature*, 295, 17
 Reuter, H.-P., & Lesch, H. 1996, *A&A*, 310, L5
 Reynolds, C. S., Di Matteo, T., Fabian, A. C., Hwang, U., & Canizares, C. R. 1996, *MNRAS*, 283, L111
 Richstone, D., et al. 1998, *Nature* 395, A14
 Sadler, E. M., Slee, O. B., Reynolds, J. E., & Roy, A. L. 1995, *MNRAS*, 276, 1373
 Turner, J. L., & Ho, P. J. 1994, *ApJ*, 421, 122
 Yi, I. 1996, *ApJ*, 473, 645
 Yi, I., & Boughn, S. P. 1998, *ApJ*, 499, 198